Novel Photonic RF Instantaneous Frequency Measurement System Using an HiBi Fiber-based Interefometer

Miguel Drummond[†], Paulo Monteiro[†¥] and Rogério Nogueira[†¥]
[†] Instituto de Telecomunicações, Campus Universitário, 3810-391 Aveiro, Portugal
Phone: +351-234377900, Fax: +351-234377901, e-mail: mvd@av.it.pt
[¥] Nokia Siemens Networks Portugal SA, 2720-093 Amadora, Portugal

***Abstract* — A novel photonic RF instantaneous frequency measurement system is proposed and experimentally demonstrated. Measurements are performed considering purely sinusoidal RF signals with frequencies up to 20 GHz and different RF input powers. A peak-to-peak frequency error down to 50 MHz is achieved for an RF frequency range of 1-18 GHz.**

I. Introduction

Modern electronic warfare such as RADAR warning receivers rely on instantaneous frequency measurement (IFM) systems with broad bandwidth and high resolution. Traditional implementations of IFM systems require electrical delay lines and mixers, thus being limited by distortion and unwanted radiation [1]. These limitations increase the cost and size of electronic IFM systems that operate up to very high frequencies.

The application of photonic microwave signal processing techniques to IFM systems is very attractive, since all-optical processing offers low losses, high time bandwidth products, light weight and immunity to electromagnetic interference [2]. The first demonstrated RADAR photonic signal processing techniques consisted on a photonic superheterodyne receiver [3], scanning receiver [4] and channeliser [5]. More recently, Nguyen and Hunter [6] proposed a photonic IFM system in which two optical carriers are modulated by a RF signal. Each carrier experiences a different amount of chromatic dispersion, leading to distinct dispersion-induced power fading after direct detection. The difference between the detected optical powers allows measuring the RF frequency. A downside of this technique is the need of high-bandwidth photodetectors. Photonic implementations of traditional electrical IFM systems were proposed in [7] and [8]. The system presented in [8] allows measuring the RF frequency and power simultaneously and independently, by taking advantage of two orthogonal DC measurements; however, it uses a higher complexity setup in comparison to [7]. Although both systems require low-bandwidth photodiodes, two electrooptic modulators (EOMs) are needed. Moreover, their modeling is complex and unambiguous frequency measurement is only possible within a limited frequency range due to oscillatory behavior. A simple approach was presented in [9], in which two optical carriers modulated by the RF signal are filtered by a sinusoidal filter. One of the carriers is centered at a maximum of the filter's response, whereas the other is centered at a minimum. The relation between the optical powers of both modulated carriers is used to measure the RF frequency, independently of the RF input power and microwave modulation index. Although this technique uses low-bandwidth photodiodes and a single EOM, it requires two optical carriers along with a multiplexer and a demultiplexer. Moreover, different wavelength drifts arise from both optical sources, leading to measurement errors. Although these previously presented systems [6-9] have reduced complexity in comparison to traditional electronic IFM techniques, they are either complex or costly.

In this paper, we propose and experimentally demonstrate a simple, cost-effective photonic IFM system based on an interferometer that operates on the polarization domain. The system uses a single optical source, avoiding the need of multiplexers/demultiplexers and different wavelength drifts. No high-bandwidth photodiodes are needed, since the output signals are average optical powers. The remaining of this paper presents a mathematical model of the device, as well the experimental validation and discussion.

II. Description and Modeling

The proposed IFM system concept is illustrated in Fig. 1. A laser diode (LD) is used to generate a continuous wave (CW) probe with linear polarization. PC1 adjusts the state of polarization (SOP) of the CW probe with the transmission axis of the MZM. The MZM is biased at the minimum transmission point, so that optical carrier suppressed modulation is achieved.

The polarization-domain interferometer consists on the PC2, PMF, PC3 and PBS. The optical carrier suppressed

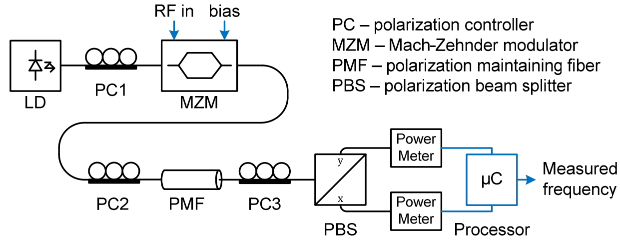

Fig. 1 Scheme of the proposed IFM system.

THRONE (PTDC/EEA-TEL/66840/2006) Fundação para a Ciência e a Tecnologia (FCT) project and BONE Network of Excellence funded by the European Commission through the 7th ICT-Framework Programme are acknowledged. M. V. Drummond was supported by FCT under the SFRH/BD/40250/2007 scholarship.

signal at the output of the MZM can be written as

$$s(t) = E_{\mathrm{CW}} e^{j\omega_{\mathrm{CW}} t} \sin[\pi z v_{\mathrm{RF}}(t)] \quad (1)$$

where E_{CW} is the amplitude of the CW probe, ω_{CW} is the angular frequency of the optical carrier, z is the microwave modulation index and $v_{\mathrm{RF}}(t)$ is the RF signal voltage, assumed to have a null average value. Considering all PCs as ideal polarization rotators and the polarization axes x and y aligned with the fast and slow axes of the PMF, respectively, one can express the signal at the output of the PMF as

$$S_{\mathrm{PMF}}(f) = S(f)\{\cos(\theta_1)\,\hat{x} + \sin\,(\theta_1) e^{-j2\pi f\tau}\hat{y}\}, \quad (2)$$

where $\hat{x}$ and $\hat{y}$ are the unit vectors along the x and y directions, $\theta_1$is the polarization rotation angle imposed by PC2 and τ represents the differential group delay (DGD) of the PMF. $S(f)$ is the Fourier transform of $s(t)$, where f represents the RF frequency. The PC3 applies another polarization rotation according to an angle of θ_2. The signal at its output is given by

$$S_{\mathrm{PC3}}(f) = S_{\mathrm{PMF}}(f)\{\hat{x}\cdot[\cos(\theta_2)\,\hat{x} + \sin(\theta_2)\,\hat{y}] + y{\cdot}\cos\theta 2y{-}\sin\theta 2x. \quad (3)$$

Using equation (2), (3) can be written as

$$\begin{aligned} S_{\mathrm{PC3}}(f) = S(f)\{&\cos(\theta_1)\cdot[\cos(\theta_2)\,\hat{x} + \sin(\theta_2)\,\hat{y}] \\ &+ \sin(\theta_1)\, e^{-j2\pi f\tau} \\ &\cdot[\cos(\theta_2)\,\hat{y} - \sin(\theta_2)\,\hat{x}]\}. \end{aligned} \quad (4)$$

The optical signals at the outputs of the PBS are given by

$$\begin{aligned} S_{\mathrm{PBS},x}(f) = S(f)\{&\cos(\theta_1)\cos(\theta_2) \\ &- \sin(\theta_1)\sin(\theta_2)\, e^{-j2\pi f\tau}\} \end{aligned} \quad (5)$$

$$\begin{aligned} S_{\mathrm{PBS},y}(f) = S(f)\{&\cos(\theta_1)\sin(\theta_2) \\ &+ \sin(\theta_1)\cos(\theta_2)\, e^{-j2\pi f\tau}\}. \end{aligned} \quad (6)$$

Hence, the x output port of the PBS consists on the destructive port of the interferometer, whereas the y output port is the constructive port. The optical signals at the outputs of the PBS depend on $S(f)$, that in turn depends on the CW probe power and microwave modulation index. To achieve a measurement independent on these parameters, an amplitude comparison function (ACF) defined as $|S_{\mathrm{PBS},x}(f)/S_{\mathrm{PBS},y}(f)|$ is used to extract the RF frequency.

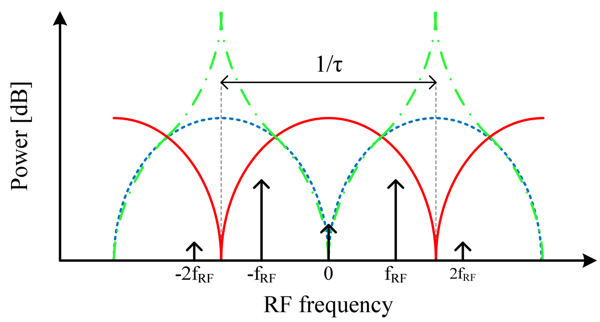

Fig. 2 Operation principle of the polarization-based interferometer. Constructive port (solid line), destructive port (dashed line) and ACF (dashed-dotted line).

Fig. 2 shows that unambiguous RF frequency measurement can be achieved for RF frequencies up to $1/2\tau$. The highest sensitivity is achieved for $\cos(\theta_1)\cos(\theta_2) = \sin(\theta_1)\sin(\theta_2)$ and $\cos(\theta_1)\sin(\theta_2) = \sin(\theta_1)\cos(\theta_2)$, which yields $\theta_1 = \theta_2 = (2k+1)\pi/4$, $k \in \mathbb{Z}$. In this case, the ACF power variation is theoretically infinite. In practice, the sensitivity is reduced by the limited accuracy in setting θ_1 and θ_2. Moreover, the extinction ratio of the output ports of the PBS and loss difference between both ports must be taken into account. Therefore, the ACF can be defined as

$$\mathrm{ACF}(f) = \left|\frac{S_{\mathrm{PBS},x}(f) + S_{\mathrm{PBS},y}(f)\cdot 10^{-\frac{\mathrm{ER}_x}{20}}}{S_{\mathrm{PBS},y}(f) + S_{\mathrm{PBS},x}(f)\cdot 10^{-\frac{\mathrm{ER}_y}{20}}}\right| \cdot \alpha, \quad (7)$$

where ER_x and ER_y are the extinction ratios of the x and y ports of the PBS, respectively. α is the loss difference between both ports. The RF frequency is extracted from the measured ACF value, through $f = \mathrm{ACF}^{-1}(f)$.

II. Experiment

An experimental setup similar to the scheme shown in Fig. 1 is considered. A CW laser with a wavelength of 1554.13 nm, 13 dBm of optical power and linewidth lower than 20 MHz is used. A MZM with 30 GHz electrical bandwidth yields an optical signal with suppressed optical carrier. Low RF input powers are considered since the MZM has a built-in electrical amplifier placed at its RF input. The electrical amplifier has an approximated small signal gain of 26 dB. The PMF produces a DGD of $\tau = 22$ ps. PC1 and PC2 are manually adjustable three-plate polarization controllers, whereas PC3 is a polarization locker that allows automatic adjustment. The extinction ratios of the PBS are $\mathrm{ER}_x = 26$ dB and $\mathrm{ER}_y = 25$ dB. An optical switch and a power meter are used instead of the two power meters of Fig. 1.The measured loss difference between both output ports of the PBS is of $\alpha = -0.6$ dB. The system calibration process is done automatically through a GPIB LabVIEW© interface that controls the RF input frequency and power, PC3 adjustment, optical switch and power meter reading. The calibration process is completed in about 20 seconds (500 ms/GHz), limited mainly by the RF frequency generator settling time and power meter reading time. All the used devices are non polarization-maintaining, except the PMF and the PBS.

A. Measured Optical Powers

Experimental results and theoretical curves derived from the mathematical model are presented in Fig. 3. θ_1 and θ_2 are optimized for each RF power to achieve the lowest peak-to-peak frequency error. Fig. 3 (a) shows that experimental optical powers deviate significantly from the theoretical predictions. This deviation is expected since $S(f)$ depends on the microwave modulation index, that in turn decreases with the increase of the RF frequency. Therefore, the measured optical powers decrease relatively to the theoretical predictions as the frequency increases. However, since the

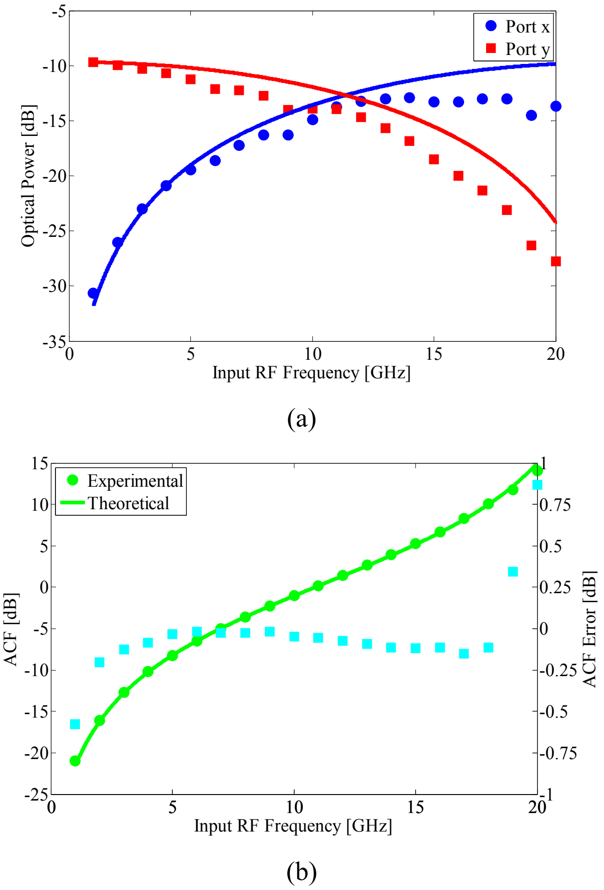

Fig. 3 IFM system results. (a) Measured optical powers and (b) ACF for a RF input power of -9 dBm. Solid lines represent theoretical curves.

ACF does not depend on $S(f)$, theoretical and experimental ACF values agree, as shown in Fig. 3 (b).

B. Measured RF frequency

The measured RF frequency and frequency errors for various RF input powers are displayed in Fig. 4. For each RF power, the peak-to-peak frequency error is lower than 200 MHz, considering a frequency range of 1 to 18 GHz. Errors increase for high RF frequencies close to $1/2\tau$ = 22.7 GHz, since the residual power of the optical carrier interferes on the measurement taken at the constructive port. This situation is illustrated in Fig. 2. The lower peak-to-peak frequency error (50 MHz) is achieved for a RF input power of -9 dBm. For lower RF input powers, the optical carrier suppression ratio decreases. In this case, the power of the optical carrier cannot be neglected relatively to the power of the RF tones, causing a slight increase of the error. On the other hand, for higher RF input powers, nonlinear distortion occurs in the modulation. The distortion arises from gain saturation of the electrical amplifier and from the nonlinear modulation transfer function of the MZM. As depicted in Fig. 2, this distortion results in increased power of the higher-order RF terms, which reduces the measurement accuracy.

The residual optical carrier derives from the bias drift and limited extinction ratio of the MZM. The MZM bias drift can

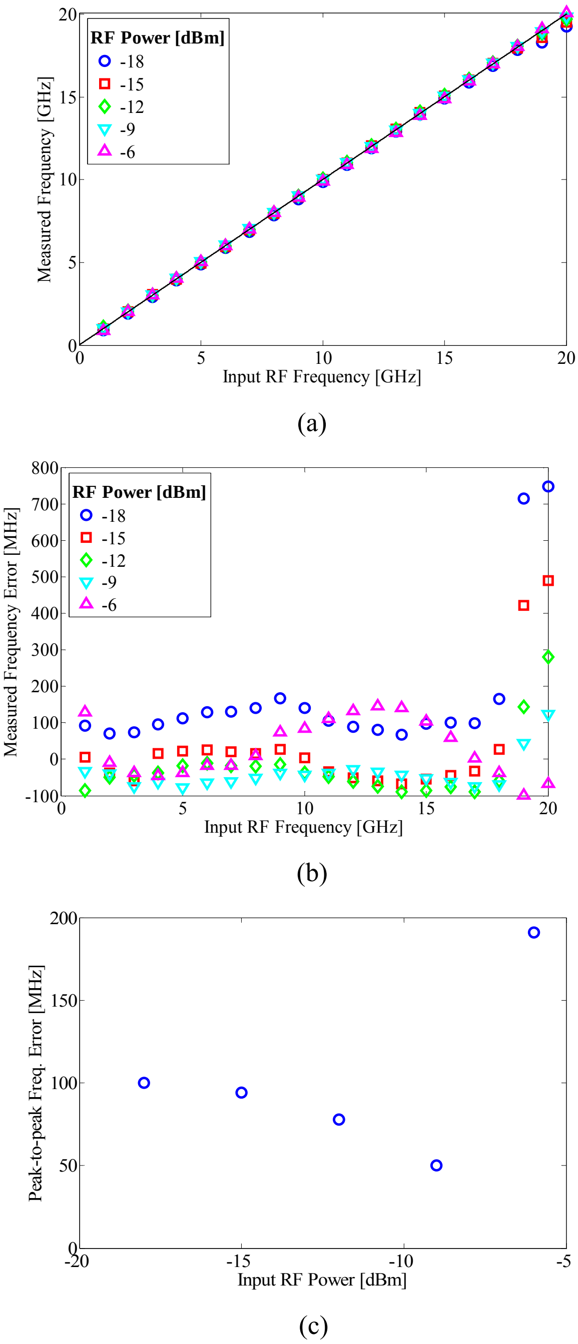

Fig. 4 (a) Measured RF frequency, (b) frequency error for various RF input powers, (c) peak-to-peak frequency error for different RF input powers considering a frequency range of 1-18 GHz.

be mitigated using an automatic bias control device. Another source of error that cannot be neglected is the instability of the signal's SOP, that can be mathematically described as a random variation of θ_1 and θ_2. The instability can be severely reduced using only PM devices.

II. CONCLUSIONS

A new photonic RF instantaneous frequency measurement system based on a polarization-domain interferometer was presented and experimentally demonstrated. Since the system takes advantage of the constructive and destructive ports of the interferometer, only a single laser source is needed. This simplifies the system design and avoids different wavelength drifts from different sources. An experimental error down to 50 MHz was achieved within a RF frequency range of 1-18 GHz. These results are comparable to the ones achieved with other cited techniques. However, in comparison with those techniques, a much simpler system is proposed. The range and resolution can be adjusted using a PMF with different DGD. The accuracy of the system can be further improved increasing the optical carrier suppression and using only PM devices.

REFERENCES

[1] M. Aikawa and H. Ogawa, "Double-sided MICs and their applications," *Microwave Theory and Techniques, IEEE Transactions on,* vol. 37, pp. 406-413, 1989.

[2] A. J. Seeds and K. J. Williams, "Microwave Photonics," *Lightwave Technology, Journal of,* vol. 24, pp. 4628-4641, 2006.

[3] A. C. Lindsay, G. A. Knight, and S. T. Winnall, "Photonic mixers for wide bandwidth RF receiver applications," *Microwave Theory and Techniques, IEEE Transactions on,* vol. 43, pp. 2311-2317, 1995.

[4] S. T. Winnall and A. C. Lindsay, "A Fabry-Perot scanning receiver for microwave signal processing," *Microwave Theory and Techniques, IEEE Transactions on,* vol. 47, pp. 1385-1390, 1999.

[5] D. B. Hunter, L. G. Edvell, and M. A. Englund, "Wideband Microwave Photonic Channelised Receiver," 2005, pp. 249-252.

[6] L. V. T. Nguyen and D. B. Hunter, "A photonic technique for microwave frequency measurement," *Photonics Technology Letters, IEEE,* vol. 18, pp. 1188-1190, 2006.

[7] N. Sarkhosh, H. Emami, L. Bui, and A. Mitchell, "Reduced Cost Photonic Instantaneous Frequency Measurement System," *Photonics Technology Letters, IEEE,* vol. 20, pp. 1521-1523, 2008.

[8] H. Emami, N. Sarkhosh, L. A. Bui, and A. Mitchell, "Amplitude independent RFinstantaneous frequency measurementsystem using photonic Hilbert transform," *Opt. Express,* vol. 16, pp. 13707-13712, 2008.

[9] H. Chi, X. Zou, and J. Yao, "An Approach to the Measurement of Microwave Frequency Based on Optical Power Monitoring," *Photonics Technology Letters, IEEE,* vol. 20, pp. 1249-1251, 2008.